Spatial partitioning of a microbial population enhances collective enzymatic defence

Nia Verdon,[1,2,3,4] Ofelia Popescu,[3,4] Simon Titmuss,[3] and Rosalind J. Allen[1,2,3]

[1] *Theoretical Microbial Ecology, Institute of Microbiology, Faculty of Biological Sciences, Friedrich Schiller University Jena, Jena, Germany*

[2] *Cluster of Excellence Balance of the Microverse, Friedrich Schiller University Jena, Jena, Germany*

[3] *School of Physics and Astronomy, University of Edinburgh, Edinburgh, UK*

[4] *Equal contribution*

Many microbes produce enzymes that modify their local environment, leading to collective benefits such as removal of antibiotic or release of environmental nutrients. Although these benefits are usually studied in large, well-mixed populations, in reality they often play out in complex, spatially partitioned geometries such as host tissue, or soil. Here, we show theoretically that partitioning into multiple small populations can strongly enhance the collective benefits of enzymatic toxin degradation. For the clinically relevant case where β-lactamase producing bacteria mount a collective defence by degrading a β-lactam antibiotic, partitioning can allow the population to survive antibiotic doses that would far exceed those required to kill a non-partitioned population. This partitioning rescue is a stochastic effect that originates from variation in the initial bacterial densities among different subpopulations. In contrast, the stochastic effects of partitioning are weaker in a model of collective enzymatic nutrient foraging. Our model suggests that treatment of a spatially complex infection showing collective resistance may be far less effective than expected based on bulk population assumptions. This may help to explain lack of correlation between lab-measured antibiotic susceptibility values and clinical treatment success.

Spatial partitioning is a common feature of microbial communities, from intracellular pathogens to colonisers of the gut lining, plant roots and soil [1–4]. Partitioning can be physical (as in gut microvilli or soil interstices), or can arise from slow diffusion of nutrients and/or signals [5]. Spatial partitioning can significantly affect microbial interactions [6–8], community assembly [9, 10] and community dynamics [1], but mechanistic understanding of these effects is lacking, since microbiological assays are usually performed on large, well-mixed bacterial populations. Here we investigate theoretically the effects of systematically partitioning a microbial population, while keeping the total population size and volume the same (Fig. 1). Using this approach, we show mechanistically how spatial partitioning can strongly affect an important class of microbial interactions: those that

are mediated by enzymatic modification of the environment.

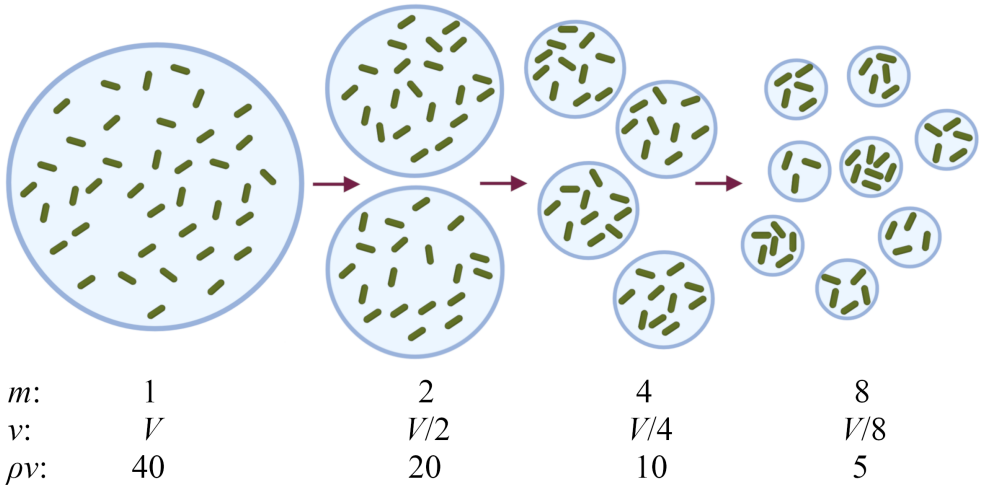

FIG. 1: **Spatial partitioning of a microbial population.** A population of microbes of density ρ, contained in volume V, is partitioned into smaller subvolumes of volume $v = V/m$. For degree of partitioning m, the average number of microbes per subvolume is ρv. Microbes are distributed stochastically among the subvolumes, so that the number of microbes in a given subvolume follows a Poisson distribution. As an exemplar, in the diagram we use $\rho v = 40$ for m=1.

Many microbes produce enzymes that modify their local environment; examples include antibiotic-degrading enzymes such as β-lactamases [11], cellulases that allow digestion of plant matter [12], hydrolases that degrade marine polysaccharides [13], sucrose digestion by yeast invertases [14], and the production of virulence factors such as elastase that cause tissue damage [15]. Enzymatic modification of the environment is often viewed as a collective behaviour, since the effects are shared by nearby microbes. Indeed, enzyme production has been analysed in the framework of social evolution theory, which addresses how enzyme production can be maintained evolutionarily in the face of cheater non-producers who reap the benefits but do not pay the cost of enzyme production [16–18]. For mixed populations of cooperators and cheaters, spatial partitioning can favour the evolution of cooperators through kin selection, although it may also increase the level of local competition between cooperators [19].

Here, we consider a clonal population, composed entirely of enzyme producers (i.e. cooperators). Our study mainly focuses on the production of β-lactamase enzymes by antibiotic-resistant bacteria [11]. These enzymes degrade β-lactams, which are among the most commonly prescribed classes of antibiotic [11, 20]. Therefore, β-lactamase producing antibiotic-resistant infections present a severe clinical problem, and improved strategies to combat them could have significant impact [11].

Consistent with the concept of β-lactamase production as a collective defence strategy against the antibiotic, β-lactamase producing bacteria often show an inoculum effect, whereby populations with high initial bacterial density survive, while those with low initial density are killed [16, 21, 22]. Recent mathematical modelling has shown that this effect can be understood as a race for survival, which depends on the relative timescales for antibiotic killing versus antibiotic degradation [23]. However, the role of spatial partitioning has not yet been considered.

Here, we present a theoretical modelling approach which we use to predict the effects of spatial partitioning on microbial enzyme-producers. Our main result is that, for microbes that engage in collective defence via enzymatic degradation of a toxin (such as β-lactam degradation), partitioning can dramatically increase the probability of survival. This suggests that antibiotic treatment of a spatially partitioned β-lactamase producing infection may be far less effective than would be expected based on the measured susceptibility (i.e. the minimum inhibitory concentration, or MIC value). In other words, partitioning can rescue an infection, allowing it to survive and regrow after the antibiotic is removed. In contrast, we find that the effects of partitioning are weaker for a microbial population that uses enzymes to boost growth by releasing nutrient from the environment. The partitioning effects predicted here are intrinsically stochastic, arising from the variability in initial population densities among the partitioned subpopulations. Therefore our study strengthens the case that stochasticity can play a key role in antibiotic efficacy [24–27].

Enzymatic modification of the environment by microbes is ubiquitous, from clinical infections to biotechnology and biogeochemistry [11–15, 28, 29]. Our study shows how the intrinsic stochasticity of population partitioning can alter the ecology of these interactions, with significant clinical implications.

Collective defence via enzymatic degradation

We first consider a microbial population that is exposed to an environmental toxin – specifically, a population of β-lactamase producing bacteria exposed to a β-lactam antibiotic. As a simple model, we suppose that the population (contained in volume V) grows exponentially if the antibiotic concentration is below a threshold a_{th} but dies exponentially if the antibiotic concentration is above the threshold. The threshold concentration a_{th} corresponds to the single-cell minimum inhibitory concentration (scMIC) [31]. In addition, the microbes produce antibiotic-degrading β-lactamase enzyme: this causes the antibiotic concentration to decrease with time. The microbial population

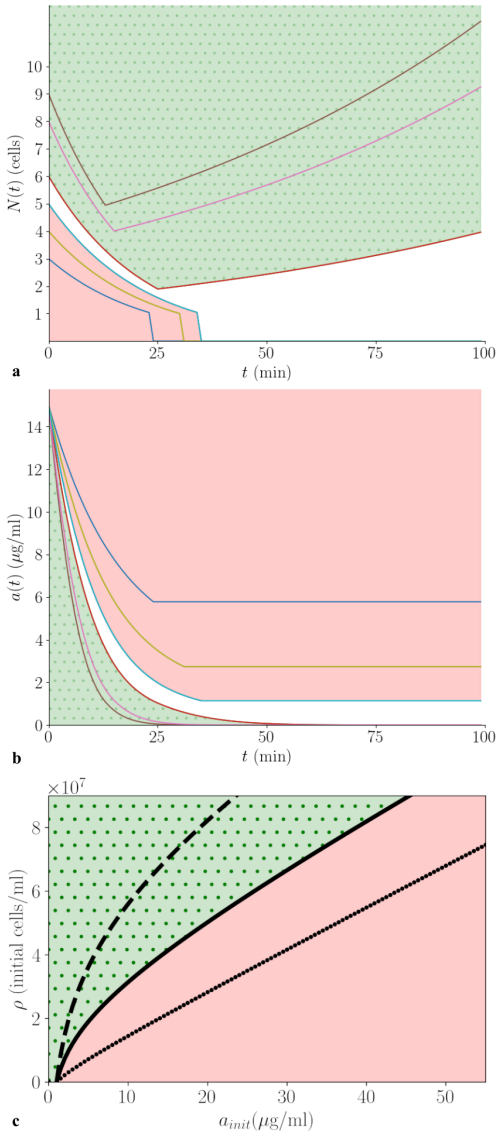

FIG. 2: **Collective enzymatic defence: population density threshold for survival**. (a,b): Predictions of the model, Eqs. 1 and 2, for the microbial population size $N(t)$ and the antibiotic concentration $a(t)$ (panels (a) and (b) respectively), for a range of values of the initial microbial population size N_{init} (coloured lines; N_{init} ranges between 3 and 9). The colour coding is consistent between (a) and (b). The red shaded region indicates death of the microbial population; the green shaded region indicates survival and regrowth of the population. The parameters are as follows: $br_{\max} = 3.5 \times 10^{-8}$ μg/cell/min [17], $K_{\text{M}} = 6.7$ μg/ml [17], $a_{\text{th}} = 1$ μg/ml [17], $a_{\text{init}} = 15$ μg/ml, $\mu = 0.01$ /min [30], $\gamma = 0.045$ /min [17], $V = 100$ pl [30]. (c): Phase diagram showing the predicted outcome (killing or survival and regrowth; red and green, respectively) as a function of initial bacterial density ρ and initial antibiotic concentration a_{init}. The lines indicate the critical density ρ^*, Eq. (3), for different values of the Michaelis-Menten parameter K_{M}: solid line $K_{\text{M}} = 6.7$ μg/ml [17], dashed line $K_{\text{M}} = 15$ μg/ml, dotted line $K_{\text{M}} = 1$ μg/ml.

size $N(t)$ is described by the following dynamical equation:

$$\dot{N(t)} = N(t)\left[\mu\theta(a_{\rm th} - a) - \gamma\theta(a - a_{\rm th})\right] , \tag{1}$$

where $\theta(x)$ denotes the Heaviside step function ($\theta(x) = 1$ if $x \geq 0$ and zero otherwise), μ is the growth rate for low antibiotic $a(t) < a_{\rm th}$, and γ is the death rate for high antibiotic $a(t) > a_{\rm th}$. The antibiotic is degraded according to:

$$\dot{a(t)} = -\frac{bN(t)}{V}\left(\frac{r_{\rm max}a(t)}{a(t) + K_{\rm M}}\right) , \tag{2}$$

where b is the number of enzyme molecules per cell (i.e. the enzyme concentration is bN/V) and each enzyme degrades antibiotic according to Michaelis-Menten kinetics with parameters $r_{\rm max}$ and $K_{\rm M}$ (note that if the enzyme remains partially or wholly within the bacterial cell, the $r_{\rm max}$ parameter also implicitly accounts for antibiotic transport across the cell boundary [23, 32]). We assume that the initial antibiotic concentration, $a_{\rm init}$, is high, $a_{\rm init} > a_{\rm th}$. Similar models have been proposed in previous work [17, 18, 23]; more detailed models of antibiotic inhibition lead to qualitatively equivalent results [23].

In our model, two distinct outcomes are possible (Fig. 2a,b). The microbial population may be killed outright, or it may reduce the antibiotic concentration below the threshold $a_{\rm th}$, and then regrow. This phenomenon has previously been described as a race for survival, since the outcome depends on the relative timescales of killing and antibiotic degradation [23]. The population will survive and regrow if its initial density is greater than a critical value ρ^* that depends on the initial antibiotic concentration [23]:

$$\rho^* = \frac{\gamma}{br_{\rm max}}\left[a_{\rm init} - a_{\rm th} + K_{\rm M}\ln\left(\frac{a_{\rm init}}{a_{\rm th}}\right)\right] . \tag{3}$$

(Fig. 2c; for derivation of Eq. 3, see the Supplementary Material). The line $\rho^*(a_{\rm init})$ defined by Eq. 3 defines an ecological phase boundary that separates regions of parameter space where the microbial population is killed from regions where it survives and regrows (Fig. 2c).

The shape of the ecological phase boundary reveals an inoculum effect (Fig. 2c): populations with a higher initial density can survive at higher initial antibiotic concentrations [21]. This arises from the collective nature of antibiotic degradation [16–18, 23]. The qualitative nature of the inoculum effect depends on the kinetic parameters of the enzyme. If K_M is small ($a_{\rm init} \gg K_M$), the phase boundary is linear (Fig. 2c, dots), but if K_M is large ($a_{\rm init} \ll K_M$), it becomes logarithmic (Fig. 2c, dashes; Eq. 3).

Under spatial partitioning, subpopulation killing is stochastic

We now ask how spatial partitioning affects the fate of a microbial population engaged in collective defence, under lethal conditions where a well-mixed population would be killed. For β-lactamase producers, this corresponds to an antibiotic concentration well above the MIC. We suppose that the total volume V, containing a population of density ρ, is partitioned into m subvolumes of volume $v = V/m$ [1] (Fig. 1). The average (initial) number of microbes per subvolume is then $\bar{N}_{\text{init}} = \rho v$. However, the subvolumes are filled stochastically, so the number of microbes $N_{i,\text{init}}$ in subvolume i is sampled from a Poisson distribution with probability $p(N_{i,\text{init}}) = e^{-\rho v}(\rho v)^{N_{i,\text{init}}}/N_{i,\text{init}}!$. Poisson statistics have indeed been observed for encapsulation of bacteria in microfluidic droplets [30, 33, 34]. Each subvolume also contains antibiotic at uniform concentration a_{init}. Neither microbes nor antibiotic can be exchanged between subvolumes, so that the microbe-antibiotic dynamics evolve independently in each subvolume. We model the dynamics in each subvolume deterministically via Eqs. 1 and 2 (although later we also consider stochastic birth-death dynamics).

In antibiotic treatment, it is important to eliminate the *entire* infection, since just a few surviving microbes can regrow and cause disease recurrence. We are therefore interested in the probability that the entire microbial population is killed, or its complement, the survival probability, which is the probability that any microbes within the population survive.

We first consider the subpopulation of microbes contained within a single subvolume v. In our model, the fate of the subpopulation is determined by its initial density (Eq. 3 and Fig. 2c); it survives if $N_{i,\text{init}}/v > \rho^*$. The probability p_s for this condition is controlled by the Poisson distribution of initial subpopulation sizes: $p_s = e^{-\rho v}\sum_{j=N^*}^{\infty}(\rho v)^j/j!$, where $N^* = \lceil \rho^* v \rceil$. Indeed, numerical simulations of the model dynamics for a single subpopulation with Poisson distributed initial population size show stochastic outcomes (Fig. 3a). For antibiotic concentrations and (average) microbial densities below the ecological phase boundary, for which the bulk, non-partitioned population is killed (Fig. 2c), some of the stochastically simulated subpopulations survive. Conversely, above the phase boundary, where a bulk population survives, some stochastically simulated subpopulations are killed (Fig. 3a). Averaging these results over many stochastic simulation runs (Fig. 3b) highlights that there is a non-zero probability of survival in regions of parameter space that are below the phase boundary and, conversely, a non-zero probability of killing in regions above the phase boundary. Therefore, stochasticity in the initial population density can change the ecological outcome for individual subpopulations.

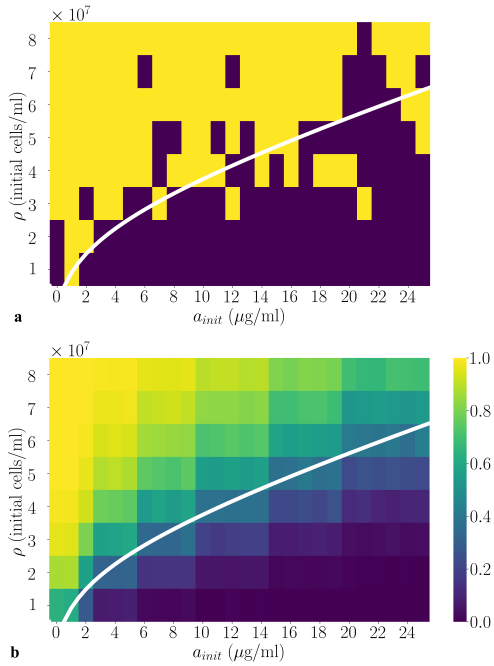

FIG. 3: **Subpopulation killing is stochastic**. (a): The model of Eqs. 1 and 2 is simulated for a single subpopulation with Poisson distributed initial population size, for a range of values of the initial antibiotic concentration a_{init} and the mean population density ρ, with $v = 100$ pl. The other parameters are $br_{\text{max}} = 3.5 \times 10^{-8} \mu$g/cell/min, $K_{\text{M}} = 6.7$ μg/ml, $a_{\text{th}} = 1 \mu$g/ml, $\mu = 0.01$/min, $\gamma = 0.045$/min (as in Fig. 2). Simulation runs in which the subpopulation is killed are shown as dark squares; those where the subpopulation survives and regrows are shown as light squares. (b): Equivalent simulations to those of (a), averaged over 1000 subpopulations for each condition. Here the probability p_s of subpopulation survival is indicated by the colour scale. In both (a) and (b) the ecological phase boundary corresponding to $\rho^*(a_{\text{init}})$ from Fig. 2c is shown as a white line.

Spatial partitioning leads to population survival via collective defence

We now consider the fate of the entire microbial population, consisting of m independent subpopulations. The probability that the entire population is killed is given by

$$1 - P_s = (1 - p_s)^m \,, \tag{4}$$

where P_s is the total population survival probability, i.e. the probability that *any* of the subpopulations survives and regrows.

Spatial partitioning strongly increases the probability of population survival. For conditions below the ecological phase boundary, for which a bulk population would be killed, simply partitioning

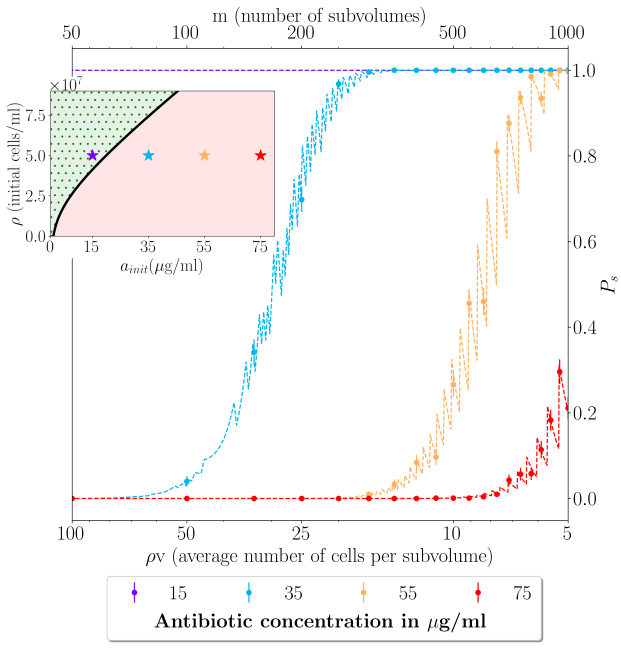

FIG. 4: **Partitioning can rescue a population in a lethal environment.** Total population survival probability P_s increases from zero to 1 as the degree of partitioning increases, for lethal parameter combinations for which a bulk population would be killed. P_s is plotted as a function of m (top axis), or the average subpopulation size ρv (bottom axis), for a range of initial antibiotic concentrations a_{init} (shown by colour) and mean population density $\rho = 5 \times 10^7$ cells/ml. The data symbols show results of numerical simulations of the model of Eqs. 1 and 2 with a Poisson distribution of initial subpopulation sizes (each data point is the mean of 1000 simulation runs; error bars show 95% confidence interval, assuming a binomial distribution), while the dashed lines show theoretical predictions obtained from Eq. 4. The zig-zagging in the theoretical lines arises because of the discreteness of individual microbes, reflected in the bound $N^* = \lceil \rho^* v \rceil$ in the sum that features in the expression for p_s. The other parameters are $br_{\max} = 3.5 \times 10^{-8} \mu$g/cell/min, $K_{\text{M}} = 6.7$ μg/ml, $a_{\text{th}} = 1 \mu$g/ml, $\mu = 0.01$/min and $\gamma = 0.045$/min (as in Fig. 2). The colour coded points in the inset show the location in the (a_{init}, ρ) phase diagram for each antibiotic concentration, relative to the survival phase boundary; a bulk population survives for 15μg/mL but dies for 35, 55 or 75 μg/mL ($\rho*$ values are 4.1×10^7, 7.4×10^7, 1.04×10^8, and 1.3×10^8 cells/ml, respectively).

the population into subvolumes (i.e. increasing m or equivalently decreasing ρv without changing the total population size or the total volume) can ensure its survival (Fig. 4). This phenomenon arises from the stochastic partitioning of microbes among the subvolumes. Because the microbes

are distributed stochastically, some subvolumes have an initial population density higher than the survival threshold ρ^* (i.e. above the phase boundary) even though the mean density ρ is below the phase boundary. For Poisson partitioning, the coefficient of variation (CV) in the initial population density increases with the degree of partitioning m (for Poisson distributed initial numbers, the subpopulation density has mean ρ and variance $\rho m/V$, hence CV= $\sqrt{m/(\rho V)}$); hence the chance of survival is increased by partitioning.

For antibiotic concentrations that are sufficient to kill the bulk population, three distinct killing regimes can be distinguished, for different degrees of partitioning. For low partitioning (small m or large ρv in Fig. 4), stochasticity is not important and the population is killed ($P_s \approx 0$). As the degree of partitioning increases, stochasticity becomes relevant and there is a significant probability of survival; here the model predicts an approximately linear relation between $\log P_s$ and the subvolume size v (Supplementary Text and Fig. S1).

In the extreme partitioning regime (very large m or very small ρv), the model predicts that the entire population survives, even for very high antibiotic concentration (Fig. 4a; see also Supplementary Fig. S3a). In this regime, the subvolume size becomes small enough that the cell density exceeds the critical value ρ^* even for a single microbe ($1/v > \rho^*$). However, our model assumes a continuous microbial population density. In this limit, since the antibiotic concentration is above the single cell MIC, an individual cell would in fact survive only if it were able to degrade antibiotic fast enough before being killed. In other words, the problem becomes a race between degradation and killing at the single cell level (see Fig. S3 for further discussion).

For populations that do survive and regrow, spatial partitioning also influences the eventual population size, since subpopulations with stochastically higher initial population size start to regrow earlier (Supplementary text and Fig. S2a).

Partitioning inhibits growth in a non-lethal environment

Interestingly, the effects of spatial partitioning are qualitatively different when the environment is non-lethal, i.e. when the initial bulk population density is above the phase boundary for survival, $\rho > \rho^*$ (green region of Fig. 2c). In this case, partitioning is actually detrimental to the microbial population. This is because some subpopulations may have initial population density below the survival threshold ρ^*; these subpopulations are killed by the antibiotic and therefore do not contribute to population growth. Numerical simulations of our model indeed confirm that the subpopulation survival probability p_s decreases with the degree of partitioning for antibiotic concentrations below

ρ^* (Fig. 5).

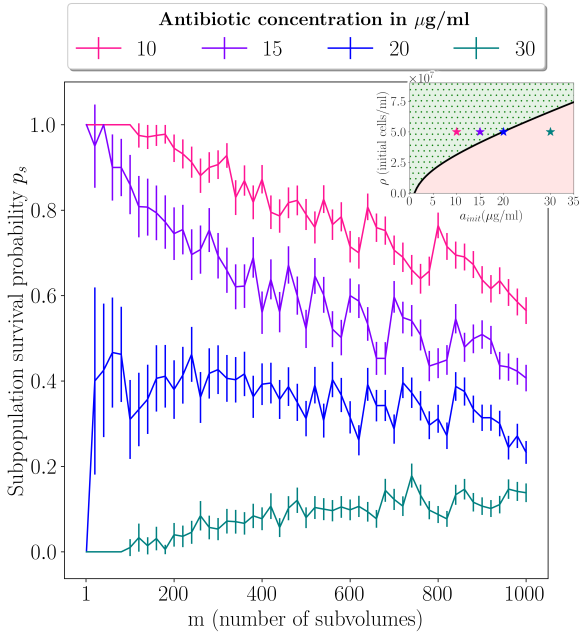

FIG. 5: **Moderate partitioning is detrimental to microbes in a non-lethal environment.** The probability p_s of survival for any given subpopulation, conditional on the subvolume being initially occupied, is plotted as a function of the degree of partitioning m. The data is obtained from numerical simulations of the model of Eqs. 1 and 2 with a Poisson distribution of initial subpopulation sizes. The mean population density $\rho = 5 \times 10^7$ cells/ml and the other parameters are $br_{\max} = 3.5 \times 10^{-8} \mu$g/cell/min, $K_{\mathrm{M}} = 6.7$ μg/ml, $a_{\mathrm{th}} = 1$ μg/ml, $\mu = 0.01$/min and $\gamma = 0.045$ /min (as in Fig. 2). For moderate degrees of partitioning, the subpopulation survival probability decreases with partitioning for low initial antibiotic concentrations, i.e. for non-lethal conditions under which a bulk population would survive. The colour coded points in the inset show the location in the $(a_{\mathrm{init}}, \rho)$ phase diagram for each antibiotic concentration, relative to the survival phase boundary. Antibiotic concentrations 10 μg/ml and 15 μg/ml are to the left of the phase boundary (non-lethal), 30 μg/ml is to the right of the boundary (lethal) and 20 μg/ml lies right on the boundary.

Demographic stochasticity can also change ecological outcomes in a partitioned population

So far, the only source of stochasticity in our analysis has been the random partitioning of microbes between subpopulations, since we used a deterministic model, Eqs. 1 and 2, for microbial

growth and death. However, in small populations intrinsic demographic stochasticity may also play a significant role [35, 36]. Repeating our analysis using the equivalent stochastic birth and death processes (simulated using a modified version of the Gillespie algorithm [37]; see Supplementary text), we find that intrinsic stochasticity in the microbial killing dynamics can also allow survival in a lethal environment (Fig. S2) [38]. For the parameter set chosen here (representative of collective β-lactamase degradation in a microfluidic droplet setup [30]), the contribution of demographic stochasticity is approximately equal in magnitude to that of stochastic partitioning, with maximal effect when both sources of stochasticity are present (Fig. S2).

Partitioning can decrease lag times for collective resource foraging via enzymatic degradation

In this work, we focused on enzymatic degradation of an antibiotic, but microbes modify their environment enzymatically in diverse ways. As a contrasting example, we also considered a microbial population which uses enzymes to release collective nutritional benefits from its environment. Examples of such behaviour include the breakdown of sucrose by the enzyme invertase produced by yeasts [14], particulate organic matter breakdown by marine bacteria [39] and the breakdown of plant cellulose by microbial cellulase enzymes [12]. We reasoned that collective resource foraging interactions might also be affected by spatial partitioning.

To probe this idea, we modified the model of Eqs. 1,2 to represent a microbial population which produces enzymes that release nutrients from the environment, facilitating growth. We suppose that the population cannot grow until the nutrient concentration exceeds a threshold, but once the nutrient threshold is reached it grows exponentially (see Supplementary text). For a bulk (non-partitioned) population, this model shows an initial lag time while the nutrient concentration is below the threshold, followed by exponential growth once the nutrient reaches the threshold.

Simulating the model for populations that are stochastically partitioned to varying degree m, we observed that partitioning decreases the lag time before population growth starts (Fig. S5). This happens because subpopulations that stochastically have a higher initial population density release environmental nutrients faster, allowing them to initiate growth earlier. In this case the ecological outcome – lag followed by growth – is the same whether or not the population is partitioned. Nevertheless, partitioning-induced lag time decrease could be relevant, for example in the case of a temporally fluctuating environment.

Discussion

Spatial partitioning is common for microbial populations in human, animal or plant host tissues, soil and other environments. Despite some pioneering studies [1, 6–10], a clear picture of how partitioning influences microbial interactions and community ecology remains to be established. Here, we showed that enzymatically mediated collective defence against a chemical toxin can be far more effective in a spatially partitioned environment than in a bulk, well-mixed environment. This is especially relevant in the context of the degradation of clinically relevant β-lactam antibiotics by β-lactamase enzymes, which are of global importance since they are the primary resistance mechanism against these antibiotics [11]. Indeed, the World Health Organisation (WHO) and US Center for Disease Control and Prevention (CDC) have identified carbapenemase-producing strains of *Pseudomonas aeruginosa*, *Acinetobacter baumannii* and Enterobacterales as critical threats [40, 41]. Our work suggests that antibiotic therapy may be even less effective against β-lactamase producing strains than suggested by their (already high) MIC values, since in a spatially partitioned environment (such as some human tissues) even doses well above the MIC may fail to eliminate an infection. The origin of this phenomenon is the pockets of high local microbial density that can arise in a partitioned environment, even when the average density is much lower. Within such high density pockets, enzyme-producing microbes are protected by their ability to rapidly degrade the antibiotic.

Interestingly, our work reveals two distinct mechanisms by which local pockets of high microbial density, leading to protection, can occur. For moderately partitioned environments, the mechanism is stochastic: if microbes are assigned randomly among different subvolumes, some subvolumes will have higher than average microbial density and thus a higher degree of protection from the antibiotic. In contrast, for extremely partitioned environments, the ecology is controlled by the shrinking subvolume size, such that the effective cell density in an occupied subvolume can be high enough for survival, even for a single microbe. However, in this case the details of degradation and death dynamics for an individual microbe, which are not included in our model, will become important.

Collective benefits among microbes are often viewed in the context of social evolution theory, where key questions concern the establishment and maintenance of cooperators (here enzyme producers) in the presence of non-producing cheaters who do not pay the fitness cost of production [42]. In social evolution theory, spatial partitioning increases the chance for genetically related organisms to share the benefits of cooperation (kin selection) but can also increase competition

among related organisms [43]. Partitioning into groups of variable size can maintain cooperators in the population via Simpson's paradox [44]. Our study shows that, even for a clonal population of cooperators, partitioning can strongly change the value of a collective benefit, especially in the case of toxin removal. Future work should explore the implications of this insight for mixed populations of cooperators and cheaters.

Our study is theoretical, and based on simple models, although more realistic models are expected to show similar behaviour [23]. Microfluidic technology increasingly allows controlled study of the dynamics of compartmentalised small microbial populations [5–7, 30, 34], including their response to antibiotics [45]. Our study provides a baseline prediction; the experimental reality may prove to be even richer, for example due to filamentation in response to antibiotic [46] and/or the de novo evolution of further resistance.

Microbial population dynamics often play out in complex environments, yet our strategies for controlling microbes are largely modelled on bulk populations and often fail. Our study reveals mechanisms that may underly such failure, and points to a need for deeper understanding of how microbial interactions and antibiotic therapy act in realistic contexts.

NV and RJA were supported by the Deutsche Forschungsgemeinschaft (DFG) via the Excellence Cluster Balance of the Microverse (EXC 2051 - Project-ID 390713860) and via SFB 1127/2 ChemBioSys - 239748522 (Project C07). NV was also funded by the EPSRC Centre for Doctoral Training in Soft and Functional Interfaces (SOFI: EP/L015536/1). OP was funded by the EPSRC Centre for Doctoral Training in Soft Matter for Formulation and Industrial Innovation (SOFI^2: EP/S023631/1). RJA was also funded by the European Research Council under Consolidator grant 682237 EVOSTRUC. The authors thank Helen Alexander, Naama Brenner, Joel Ching Kuma Mbanghanih, Diana Fusco, Tatjana Malycheva, Daniel Taylor and Stefan Schuster for valuable discussions. For the purpose of open access, the author has applied a Creative Commons Attribution (CC BY) licence to any Author Accepted Manuscript version arising from this submission.

---

[1] Wu, F. *et al.* Modulation of microbial community dynamics by spatial partitioning. *Nature Chem. Biol.* **18**, 394–402 (2022).

[2] Edwards, J. *et al.* Structure, variation and assembly of the root-associated microbiomes of rice. *Proc. Natl. Acad. Sci. USA* **112**, 911–920 (2015).

[3] Bickel, S. & Or, D. Soil bacterial diversity mediated by microscale aqueous-phase processes across

biomes. *Nat. Commun.* **11**, 116 (2020).

[4] Welch, J. L. M., Hasegawa, Y., McNulty, N. P., Gordon, J. I. & Borisy, G. G. Spatial organization of a model 15-member human gut microbiota established in gnotobiotic mice. *Proc. Natl. Acad. Sci. USA* **114**, 9105–9114 (2017).

[5] Dal Co, A., van Vliet, S., Kiviet, D. J., Schlegel, S. & Ackermann, M. Short-range interactions govern the dynamics and functions of microbial communities. *Nature Ecol. Evol.* **4**, 366–375 (2020).

[6] Boedicker, J. Q., Vincent, M. E. & Ismagilov, R. F. Microfluidic confinement of single cells of bacteria in small volumes initiates high-density behavior of quorum sensing and growth and reveals its variability. *Angew. Chemie Int. Ed.* **48**, 5908–5911 (2009).

[7] Connell, J. L., Kim, J., Shear, J. B., Bard, A. J. & Whiteley, M. Real-time monitoring of quorum sensing in 3D-printed bacterial aggregates using scanning electrochemical microscopy. *Proc. Natl. Acad. Sci. USA* **111**, 18255–18260 (2014).

[8] Geyrhofer, L. & Brenner, N. Coexistence and cooperation in structured habitats. *BMC Ecol.* **20**, 14 (2020).

[9] Hansen, R. H. *et al.* Stochastic assembly of bacteria in microwell arrays reveals the importance of confinement in community development. *PLoS One* **11**, e0155080 (2016).

[10] Hsu, R. H. *et al.* Microbial interaction network inference in microfluidic droplets. *Cell Systems* **9**, 229–242 (2019).

[11] Tooke, C. L. *et al.* β-lactamases and β-lactamase inhibitors in the 21st century. *J. Mol. Biol.* **431**, 3472–3500 (2019).

[12] Thapa, S. *et al.* Microbial cellulolytic enzymes: diversity and biotechnology with reference to lignocellulosic biomass degradation. *Rev. Environ. Sci. Biotechnol.* **19**, 621–648 (2020).

[13] Arnosti, C. Microbial extracellular enzymes and the marine carbon cycle. *Annu. Rev. Mar. Sci.* **3**, 401–425 (2011).

[14] Gore, J., Youk, H. & van Oudenaarden, A. Snowdrift game dynamics and facultative cheating in yeast. *Nature* **459**, 253–256 (2009).

[15] Galloway, D. R. *Pseudomonas aeruginosa* elastase and elastolysis revisited: recent developments. *Mol. Microbiol.* **5**, 2315–2321 (1991).

[16] Vega, N. M. & Gore, J. Collective antibiotic resistance: mechanisms and implications. *Curr. Opin. Microbiol.* **21**, 28 (2014).

[17] Yurtsev, E. A., Chao, H. X., Datta, M. S., Artemova, T. & Gore, J. Bacterial cheating drives the population dynamics of cooperative antibiotic resistance plasmids. *Mol. Syst. Biol.* **9**, 683 (2013).

[18] Mizrahi, S. P., Goyal, A. & Gore, J. Community interactions drive the evolution of antibiotic tolerance in bacteria. *Proc. Natl. Acad. Sci. USA* **120** (2022).

[19] Tekwa, E. W., Nguyen, D., Loreau, M. & Gonzalez, A. Defector clustering is linked to cooperation in a pathogenic bacterium. *Proc. R. Soc. B* **284**, 20172001 (2017).

[20] Bush, K. & Bradford, P. A. β-lactams and β-lactamase inhibitors. *Cold Spring Harb Perspect Med.* **6**,

a025247 (2016).

[21] Brook, I. Inoculum effect. *Rev. Inf. Dis.* **11**, 361–368 (1989).

[22] Meredith, H. R., Srimani, J. K., Lee, A. J., Lopatkin, A. J. & You, L. Collective antibiotic tolerance: mechanisms, dynamics and intervention. *Nat. Chem. Biol.* **11**, 182 (2015).

[23] Geyrhofer, L. *et al.* Minimal surviving inoculum in collective antibiotic resistance. *mBio* **14**, 02456–22 (2023).

[24] Balaban, N. Q., Merrin, J., Chait, R., Kowalik, L. & Leibler, S. Bacterial persistence as a phenotypic switch. *Science* **305**, 1622–1625 (2004).

[25] Coates, J. *et al.* Antibiotic-induced population fluctuations and stochastic clearance of bacteria. *eLife* **7**, e32976 (2018).

[26] Deris, J. B. *et al.* The innate growth bistability and fitness landscapes of antibiotic-resistant bacteria. *Science* **342**, 1237435 (2013).

[27] Alexander, H. K. & MacLean, R. C. Stochastic bacterial population dynamics restrict the establishment of antibiotic resistance from single cells. *Proc. Natl. Acad. Sci. USA* **117**, 19455–19464 (2020).

[28] Zhang, S., Mukherji, R., Chowdhury, S., Reimer, S. & Stallforth, P. Lipopeptide-mediated bacterial interaction enables cooperative predator defence. *Proc. Natl. Acad. Sci. USA* **118**, e2013759118 (2021).

[29] Hermenau, R., Kugel, S., Komor, A. J. & Hertweck, C. Helper bacteria halt and disarm mushroom pathogens by linearizing structurally diverse cyclolipopeptides. *Proc. Natl. Acad. Sci. USA* **117**, 23802—-23806 (2020).

[30] Taylor, D., Verdon, N., Lomax, P., Allen, R. J. & Titmuss, S. Tracking the stochastic growth of bacterial populations in microfluidic droplets. *Phys. Biol.* **19**, 026003 (2022).

[31] Artemova, T., Gerardin, Y., Dudley, C., Vega, N. M. & Gore, J. Isolated cell behavior drives the evolution of antibiotic resistance. *Mol. Sys. Biol.* **11**, 822 (2015).

[32] Dugatkin, L. A., Perlin, M., Lucas, J. S. & Atlas, R. Group-beneficial traits, frequency-dependent selection and genotypic diversity: an antibiotic resistance paradigm. *Proc. R. Soc. B* **272**, 79–83 (2005).

[33] Collins, D. J., Neild, A., DeMello, A., Liu, A.-Q. & Ai, Y. The Poisson distribution and beyond: methods for microfluidic droplet production and single cell encapsulation. *Lab Chip* **15**, 3439–3459 (2015).

[34] Barizien, A., Suryateja Jammalamadaka, M. S., Amselem, G. & Baroud, C. N. Growing from a few cells: combined effects of initial stochasticity and cell-to-cell variability. *J. R. Soc. Interface* **16**, 20180935 (2019).

[35] Allen, R. J. & Waclaw, B. Bacterial growth: a statistical physicist's guide. *Rep. Prog. Phys.* **82**, 016601 (2019).

[36] Khatri, B., Free, A. & Allen, R. J. Oscillating microbial dynamics driven by small populations, limited nutrient supply and high death rates. *J. Theor. Biol.* **314**, 120–129 (2012).

[37] Gillespie, D. T. A general method for numerically simulating the stochastic time evolution of coupled

chemical reactions. *J. Comp. Phys.* **22**, 403–434 (1976).

[38] Teimouri, H. & Kolomeisky, A. B. Theoretical investigation of stochastic clearance of bacteria: first-passage analysis. *J. R. Soc. Interface* **16**, 20180765 (2019).

[39] Ebrahimi, A., Schwartzman, J. & Cordero, O. X. Cooperation and spatial self-organization determine rate and efficiency of particulate organic matter degradation in marine bacteria. *Proc. Natl. Acad. Sci. USA* **116**, 23309–23316 (2019).

[40] Tacconelli, E. Global priority list of antibiotic-resistant bacteria to guide research, discovery, and development of new antibiotics. Tech. Rep., World Health Organization (2017).

[41] CDC. Antibiotic resistance threats in the United States. Tech. Rep., U.S. Department of Health and Human Services (2019).

[42] West, S. A., Griffin, A. S., Gardner, A. & Diggle, S. P. Social evolution theory for microorganisms. *Nat. Rev. Microbiol.* **4**, 597–607 (2006).

[43] Peña, J.&Nldeke, G.Groupsizeeffectsinsocialevolution. J. Theor. Biol.**457**, 211 − −220(2018).

[44] Chuang, J. S., Rivoire, O. & Leibler, S. Simpson's paradox in a synthetic microbial system. *Science* **323**, 272–275 (2009).

[45] Scheler, O. *et al.* Droplet-based digital antibiotic screen reveals single-cell clinal heteroresistance in an isogenic bacterial population. *Sci. Rep.* **10**, 3282 (2020).

[46] Zhao, X., Ruelens, P., Farr, A. D., de Visser, A. G. M. & Baraban, L. Population dynamics of cross-protection against β-lactam antibiotics in droplet microreactors. *Front. Microbiol.* **14**, 1294790 (2023).